International Journal of Multiphysics
Volume 18, No. 3, 2024
ISSN: 1750-9548

Role of Multi-Slice Computed Tomography in the Acute Abdomen

Rahmah Muhammad Mahammoud Hurreh, Mohamad H. Abowarda, Hanan Abdelhamed Ismael, Enas Moustafa Ibrahim

Radiology Department, Faculty of Medicine, Zagazig University, Egypt

***Corresponding author:** Rahmah Muhammad Mahammoud Hurreh

Email: Rahmambh@gmail.com,

Abstract:

Acute abdominal pain represents one of the most common and challenging presentations in emergency departments, often requiring rapid and accurate diagnosis to guide appropriate management. Clinical examination and laboratory investigations alone may be insufficient to determine the underlying cause, particularly in non-traumatic cases with overlapping symptoms. Multi-slice computed tomography (MSCT) has emerged as a highly valuable imaging modality due to its high spatial resolution, rapid acquisition, and ability to provide comprehensive evaluation of abdominal organs. The use of contrast-enhanced MSCT has significantly improved diagnostic accuracy, enabling early detection of life-threatening conditions and reducing unnecessary surgical interventions.

Keywords: Multi-slice computed tomography; Acute abdomen; Non-traumatic abdominal pain; Contrast-enhanced CT; Emergency radiology.

Introduction:

Acute abdominal pain is one of the most common causes of emergency department visits and hospital admissions worldwide. It represents a broad clinical spectrum of conditions ranging from benign, self-limiting disorders to life-threatening surgical emergencies. The nonspecific nature of clinical presentation in many patients often makes accurate diagnosis challenging, and delays in diagnosis may result in increased morbidity, mortality, and healthcare costs. Therefore, rapid and precise diagnostic evaluation is essential for optimal patient management and outcome **(1).**

Although clinical assessment and laboratory investigations remain fundamental components in the evaluation of patients with acute abdomen, they are frequently insufficient to establish a definitive diagnosis. Conventional imaging modalities such as plain abdominal radiography and ultrasonography have traditionally been used as first-line tools; however, their diagnostic accuracy is limited by factors such as operator dependency, patient obesity, bowel gas, and restricted visualization of retroperitoneal structures. These limitations have driven the increasing reliance on advanced cross-sectional imaging techniques in emergency radiology **(2).**

Multi-slice computed tomography has revolutionized the diagnostic approach to non-traumatic acute abdominal conditions. With its rapid acquisition, high spatial resolution, and multiplanar reconstruction capabilities, contrast-enhanced MSCT enables comprehensive evaluation of abdominal organs, bowel, mesentery, and vascular structures in a single examination. Numerous studies have demonstrated that MSCT significantly improves diagnostic accuracy, facilitates early detection of complications, reduces negative surgical exploration, and plays a crucial role in guiding appropriate medical or surgical management in patients presenting with acute abdomen **(3).**

Principles of Spiral CT

The advent of spiral CT, also called helical (volume) has undoubtedly revolutionized clinical imaging. The use of spiral technology has enhanced established CT applications by the minimization of motion related artifacts, misregistration artifacts and the construction of overlapping images without additional radiation

exposure (**4**). The generation of 3 dimensional (3D) images from transaxial images acquired in a single breath hold is now possible. Spiral CT involves synchronized translatory movement of the patient through the gantry while the x-ray source rotates such that uninterrupted data acquisition is achieved throughout the region of interest. The x-ray source traces a helix on the patient surface, resulting in a block of data, not isolated slices as happens in traditional axial scanning. The acquisition of volumetric data permits data manipulation options not previously obtainable with conventional axial scanning (**5**).

According to **Romans (4**) for spiral CT to be practical, many complications associated with conventional axial CT had to be overcome. The main developments leading to its progress were **1)** x-ray gantries with a slip ring technology, **2)** more efficient tube cooling, **3)** superior x-ray output (i.e., increased mA capability), **4)** smoother table movement, **5)** software that adjusts for table motion, **6)** better raw data management, and **7)** more efficient detectors.

Difference between MDCT and conventional Spiral CT

Up until the 1990s all commercial scanners contained numerous detector elements aligned in a single row. This single row design was used in both the third and fourth generation scanners. The detector elements were arranged in an arch in third, and a complete ring in the fourth generation CT units. The detector elements in conventional spiral CT are wide in the z-axis, typically 15mm and the beam collimation controls the slice thickness. This means that the width of the detector elements in the z-direction place an upper limit on the slice thickness possible. Apparently, opening of the collimators beyond this does not increase the slice thickness any further, rather it only increases scatter and radiation dose to the patient. Radiation emitted from a tightly collimated x-ray source produces a fan beam that covers the entire field of interest in a single direction. Therefore each 360 degrees gantry rotation produces only one slice. The area of patient anatomy to be scanned can be calculated by multiplying the slice increment selected by the number of slices acquired (**5**).

Modern MDCT systems continue to use many detector elements arranged in a row, but instead of a single row, they range from 4 to 320 parallel rows. Consequently, in MDCT a single rotation can produce multiple slices. Furthermore, MDCT delivers lengthier and faster *z* axis coverage per 360 degrees gantry rotation, which increases volume coverage per unit time. The Toshiba Aquilion One Vision Edition, is armed with a gantry rotation of 0.275 seconds and 320 detector rows (640 unique slices) covering 16 cm in a single rotation, with the industry's thinnest slices at 500 microns (0.5 mm). In these systems slice thickness determined by both x-ray beam width and detector configuration. In addition, the multidetector channels can be used for either axial or helical data acquisitions (**4**).

Essentially, MDCT scanner contrasts from the single-slice CT scanner mainly in terms of design of detector assembly. Extreme MDCT (i.e. 256 and 320 rows) has been developed with the hope of exploring the possibility of achieving 0.16-mm spatial resolution offered by typical fluoroscopy tubes. However, extreme MDCT angiography (CTA) has been shown to offer excellent sensitivity and negative predictive value for functional stenosis (**6**). The major advantage of extreme MDCT scanners is their capacity to image the heart, brain, and many other organs in a single rotation (**4).**

Slip ring technology

Before helical scanning systems, CT gantries moved first in one direction, then stopped as the table moved to the next position. CT examination times were dominated by interscan delays. After each 360°rotation, cables joining rotating components (x-ray tube and, if third generation, detectors) to the rest of the gantry required that rotation stop and reverse direction. Cables were spooled onto a drum, released during rotation, and then respooled during reversal. Scanning, braking, and reversal required at least 8–10 s, of which only 1–2 were spent acquiring data. The result was poor temporal resolution (for dynamic contrast enhancement studies) and lengthy procedure times (**5**).

To eliminate interscan delays, required non-stop rotation of the gantry a capability that was made possible by slip ring technology. Slip rings use a brush like device to deliver continuous electrical power and electronic communication across a rotating surface. They allow the gantry frame to rotate nonstop in the same direction, excluding the need to straighten twisted system cables. The x-ray tube can also reach much higher speeds, thereby

reducing the time needed for each data acquisition. Before the use of slip rings it took CT scanners from 2 to 5 seconds to complete a single rotation, whereas a slip ring scanner can achieve sub second times **(4)**.

Detector designs

The detector array design in multiple-row detector CT differs with each manufacturer. However, with the introduction of 16-channel CT scanners, all CT manufacturers adopted a fairly identical design for their x-ray detectors. CT manufacturers also established similar detector pattern designs for 32-, 40-, 64 and 128-channel detector systems. There are basically three designs namely matrix, adaptive and hybrid designs (**5**).

(a). Matrix Detectors.

Also called uniform or mosaic detectors. In this design the parallel rows are of equal size, for example the Toshiba Acquisition 64 contains 64 detectors all of which are 0.5mm thick.

(b). Hybrid detectors.

These have a combination of two discrete detector element sizes. This detector design has a number of narrow detector elements in the center of the detector and a different number of wider detectors (usually double the width of the narrow detectors) on both sides of the span of narrow detectors. The number of narrow and wider detectors can vary. For example, the Siemens Sensation 64 spots 32 central 0.6mm detectors and 8 1.2mm peripheral detectors. Using the z-flying focal spot technology (z-Sharp) it then produces 64 slices (**5**).

(c). Adaptive detectors.

They are also called non-uniform or variable detectors. In this design, the element sizes are variable and not uniform. There are smaller detectors centrally and relatively larger ones peripherally. For example, one of the Siemens designs has central 1mm, then 2.5mm and 5mm peripherally. When combined with a physical post patient collimator, signals from these detectors can be combined to form several values of image thickness in a way that increases detector efficiency over that of uniform detectors. This enhancement is a product of the reduced proportion of dead space due to the divisions (cell walls) between detector elements.

Isotropic Imaging

Every CT slice symbolizes a particular plane in the patient's body. The thickness of the slice is called the z axis; i.e. the z axis symbolizes the slice thickness. The slice thickness is selected by the radiographer and is determined by both collimators and detector configuration in MDCT. Furthermore, data from the CT slice is sectioned into the width indicated by X and the height is specified by Y (**4**). A **pixel** (or **pel** or **picture element**) can refer to either the smallest isolated element of the physical display or to the smallest element of the image. A combination of thousands of pixels generates the CT image that shows on the CT monitor. If the *Z* axis is considered, the outcome is a cube, rather than a square. This cube is what is called a voxel (volume element). A matrix is formed from the rows and columns of pixels. Newer CT systems use 1,024 matrix size, which translates to 1,024 rows of pixels down and 1024 rows of pixels across. These CT scanners permit for very thin slice thickness; often the aim is to produce isotropic voxels or to achieve isotropic imaging.

An isotropic voxel is a cube, measuring the same in the *x, y,* and *z* directions. When the imaging voxel is a replica in size in all dimensions there is no loss of information when data are reformatted in a different plane. Isotropic imaging is when multiplanar reconstruction (MPR) images can be produced in any plane with identical spatial resolution as the original acquisition. Very thin slices are required; for example 1mm for head CT. From the thin slices coronal, sagittal, curved or oblique sections can be obtained using the same data set, rather than acquiring extra sections. This enhances patient comfort, decreases radiation and offers these planes of imaging in patients where such images were formerly impossible to obtain. Despite all the advantages of isotropic imaging, there is a trade off in the form of radiation dose to the patient. Dose increases of approximately 100% in 4-16 slice CT machines and 15-28% in 40 slice systems. However, isotropic imaging is justifiable in 64 slice and above systems (**5**).

Radiation Dose Considerations

The advent of MDCT has caused a tremendous rise in the number of CT examinations performed per year. This increase has made CT one of the largest contributors of medical radiation dose, with a six fold upsurge in the per-capita annual effective dose from medical procedures in the United States alone, from 0.5 mSv in 1980 to 3 mSv in 2006 (**7**). In the United Kingdom and Sweden, CT scans made up 60% and 58% respectively, of the collective dose to patients from medical diagnostic exposures by the 2010. There has been rising concerns about the radiation dose from CT. In response, radiologists, radiographers, medical physicists, and manufacturers have employed many examination protocols, software and hardware adjustments to diminish CT radiation dose. The most popular methods employed by physicists and manufacturers include; Automatic Exposure control (AEC) and Automatic Tube Current Modulation (ATCM) (**8**).

i. Automatic Exposure control (AEC)/Automatic Tube Current Modulation (ATCM).

AEC are devices designed to deliver a constant optical density irrespective of tissue thickness, composition, or failure of the reciprocity law (**9**). Currently, practically all CT systems are equipped with AEC systems with tube current modulation in three dimensions (ATCM). Although, each of these systems has modified specifications and operates somewhat differently, their main principle is to manage the required image quality and radiation dose in a reproducible manner by adapting the tube current to the patients shape, size and attenuation. If an AEC/ATCM system is correctly optimized it can reduce patient dose by about 20-40% while maintaining adequate image quality for confident diagnosis. The benefits of AEC/ATCM include; improved control of the dose absorbed by the patient, better consistency of image quality among patients, reduced load on the x-ray tube, which extends lifetime and reduction of some image artifacts. Several studies have confirmed the efficacy of AEC/ATCM systems by using standardized phantoms and performing clinical work (**9**).

Greffier *et al.,* (10) report that in chest paediatric MDCT, the use of AEC with Iterative Reconstruction permits one to obtain a substantial dose reduction while maintaining constant image quality indices.

The first prerequisite for the operation of AEC/ATCM is the determination of patient attenuation. This is done mainly from scan projection radiographs (SPRs), called variously topogram, scout, surview or scanogram by different manufacturers, which contain information on both patient tissue sizes and attenuations. The modifications may be based on a single SPR using predictive calculations of the difference in AP/lateral dimensions or two SPRs. Siemens AEC is called CARE Dose4D and has three constituents to mA-modulation: 1) patient size adaptation, 2) z-axis modulation to account for variances in patient attenuation along the z- axis, and 3) on-the-fly angular modulation to account for differences in patient attenuation in the lateral and AP dimensions (**11**).

CARE Dose4D can use either two SPRs or a single SPR and adjust the angular mA based on online feedback measurements during each tube rotation. The attenuation profile measurements made from the previous 180° view are used to calculate the angular modulation of the mA (**5**).

For all CT scanners, the typical attenuation values for each rotation from the SPR are changed into water equivalent thicknesses (WETs), and the mA is set automatically at each Z-position to achieve a selected image quality reference based on the WET using proprietary algorithms. The variation may be in the form of step changes in mA for every AP and lateral quadrant, or a sinusoidal interpolation between AP and lateral values. Thus the exposure, which is determined by the product of tube current (mA) and exposure time (s) or mAs, is varied along and around the body to match the tissue attenuation for each patient, and the current modulation will follow different patterns, depending on body shape (**12).**

Low dose CT

Radiation dose delivered to patients can be reduced by lowering the exposure parameters such kilo-voltage (kV) or tube current (mA) during image acquisition. Studies have shown that there is no significant difference in the image quality obtained with either a lowered kV or tube current. There is however, no consensus on which level of dose is considered a low dose and the factors affecting dose in CT are different, such as tube

voltage (kVp, kilovolt peak), tube current (mA, milliampere) and tube speed rotation (s, second). LDCT has been used successfully in lung cancer screening programs with average effective doses of 2mSv (**5).**

Speelman and Davidson (13), demonstrated that LDCT can be used in detection of hepatic metastases.

Filters used in CT

Compensating filters are used to shape the x-ray beam. They lower the radiation dose to the patient and help to decrease image artifacts. Radiation emitted by CT x-ray tubes is polychromatic. Filtering the x-ray beam helps to reduce the range of x-ray energies that reach the patient by removing the long-wavelength (or "soft") x-rays. These long-wavelength x-rays are readily absorbed by the patient, therefore they do not contribute to the CT image but do contribute to the radiation dose to the patient. In addition, creating a more uniform beam intensity improves the CT image by reducing artifacts that result from beam hardening. Different filters are used when scanning the body than when scanning the head. Human body anatomy typically has a round cross section that is thicker in the middle than in the periphery. Hence, body-scanning filters are used to reduce the beam intensity at the periphery of the beam, corresponding to the thinner areas of a patient's anatomy. Because of their shape they are often referred to as bow tie filters (**4).**

The drawback of the current bowtie filter is that the attenuation profile it produces is fixed and cannot be adaptively altered with the gantry rotation. Although modern CT scanners have a few bowtie filters for different applications, these filters are not personalized and must be fixed for an entire scan (**14).**

Clinical Applications of MDCT

CT Colonography (CTC)

Also called virtual endoscopy is a cutting edge innovation in CT. CTC is a tool for detecting colorectal neoplasms that uses volumetric CT data. The CT data set is obtained after a patient has undergone a bowel washout and an air enema. This is performed by helical CT with thin slices. Volumetric data is then analyzed using CTC software which provides an interactive display of multiplanar two dimensional (2D) and three dimensional (3D) images of the colon. The most common tool used in CTC is the "Fly through" technique which mimics the appearance observed by an endoscope. The performance of CTC has been assessed in patients with known or suspected polyps and has been shown to be more effective than other tests (**5**).

A clinical study has reported that the sensitivity and specificity of CTC averaged 75% and 90% in patients with adenomas 10 mm in diameter or greater. The risk of malignancy is 10% for adenomas 10 to 20 mm in diameter and increases to at least 30% in adenomas larger than 20 mm in diameter (**15).**

CTC can also be used as a screening tool in asymptomatic adults. It is less invasive, less time- consuming, and less expensive than optical colonoscopy and can be at least as effective. **Svensson *et al.,* (16**) stated that CTC is better tolerated by patients than conventional colonoscopy. The advantages of CTC over Barium enema are the lack of superimposed structures and the availability of problem solving techniques. The American Cancer Society in 2018 added CTC as one of the screening options for colorectal cancer because extrapolation from Randomised Control Trials of sigmoidoscopy demonstrated mortality reduction. Furthermore, CTC sensitivity and specificity for cancer and advanced adenomas is similar to conventional colonoscopy (**5**).

Despite CTC being reported to be a safe, noninvasive method for examining the entire colon, in isolated cases bowel distention can cause bowel perforation. In addition, residual stool is a common finding at CTC and represents a significant source of pitfalls. Stool can either simulate or obscure colonic lesions and lead to interpretation or perception errors. Three-dimensional virtual colonoscopy mimics an endoscopic examination. Therefore, it is likely to miss lesions located in "blind spots" for the virtual camera if 3D virtual colonoscopy is used for the primary search process (**17).**

Post-processing techniques and reporting

Three main post-processing techniques are used. Multi-planar reconstructions (MPRs) are useful for interpretation of abdominal diseases as they allow the scanned volume to be viewed in any arbitrary plane

interactively determined by the viewer. These reconstructions are especially useful when tubular structures, such as vessels, ureters, and bowel, are followed. Maximum intensity projections (MIPs) are obtained by the projection onto an image plane of the highest attenuation voxels encountered through a volume, which allows for evaluation of structures that are not lying in a single plane. MIP is useful for CT angiography and CT urography (**18**).

Main disadvantages are that vessels adjacent to bones may be obscured. The reconstruction of volume-rendered (VR) images is particularly helpful for visualisation of complex anatomy and pathology of visceral vasculature and best delineates a tortuous course of vessels and small branches compared with MPR or axial images alone (**19).**

The evaluation of abdominal CT studies is routinely performed on dedicated workstations by interactive viewing. The following algorithmic approach is helpful in most patients (**20):**

- Initial viewing of the axial source images in scroll-through mode is mandatory.
- Interactive viewing in the coronal plane is usually done in all patients, and in the majority of cases axial and coronal images are sufficient for evaluating abdominal disease.
- Additional sagittal, oblique, or curved planar reconstructions may facilitate diagnosis in equivocal findings.
- In suspected vascular or ureteral disease, MIPs are usually reconstructed in dedicated planes and slab-thickness is adapted to include the area of interest.
- In suspected vascular pathology, VR images may be helpful in understanding complex vascular pathology and reporting the results to clinical colleagues.
- Finally, all pathological conditions should be verified again on the axial images to avoid false positive findings, because all post-processing techniques have the potential hazard of loss of valuable information when improperly used.

The major disadvantage of MDCT examinations is the large number of data and images that are produced, making efficient and accurate reporting on hard-copy images difficult. In addition, it is obviously not cost-effective to hard-copy all images. For reporting, axial slices with a thickness of 5 mm and an increment of 10 mm are printed on hard copies. In ureteral stone disease, reporting on hard copies may be limited to coronal reformations and coronal MIPs. Additional MPR, MIP, and VR reconstructions are not essential for the reporting of every examination and should be limited in the further evaluation of an area of abnormality, particularly when axial images alone make interpretation difficult (**21).**

Examination protocols

Patients presenting with acute abdominal pain in the emergency department are scanned on a 16-row MDCT scanner (Sensation 16, Siemens, Forchheim, Germany) using the following parameters: tube voltage 120 kV, tube current 225 mAs, slice collimation 16 mm×0.75 mm, pitch 1.0. Routinely, slices with a thickness of 2.0 mm (increment 1.0 mm) and a medium soft-tissue reconstruction kernel (B30f) are used for evaluation. Based on the working clinical diagnosis, optimising the acquisition parameters is essential to maximise diagnostic accuracy. For instance, narrow collimation (1 mm slice thickness, 0.5 mm increment) is used for CT angiography (**22).**

MSCT in the acute abdomen

MSCT systems have enabled faster and superior evaluation of the acute abdomen. Greater volume coverage and thinner slice acquisition have been achieved without significant increases to patients' radiation burden. Such advances in CT technology have enabled images to be acquired in multiple phases with submillimeter resolution. The routine use of isotropic, multiplanar reconstructions at dedicated CT workstations is also improving the accuracy of MSCT and speeding interpretation. This may be particularly useful when evaluating tubular structures, such as bowel or blood vessels (**23).**

Right upper quadrant pain

The most common cause of acute abdominal pain in the right upper quadrant (RUQ) is acute cholecystitis, especially in the elderly patient. Although sonography is the preferred imaging method, patients with acute RUQ pain often undergo CT as initial examination. CT may than be useful in diagnosing acute, complicated, calculous or acalculous cholecystitis when the diagnosis is difficult to establish by sonography. If CT is the initial imaging modality performed in a patient with abdominal pain, recognition of typical CT findings may eliminate the need for any additional imaging modality, thus facilitating appropriate and expedient management. For most patients, a standard CT protocol with intravenous administration of contrast agent and portal venous phase imaging is adequate (**24).**

The most sensitive CT findings in acute cholecystitis are mural thickening of more than 3 mm with increased attenuation in the setting of a distended gall bladder. Other findings include peri-cholecystic fluid or haziness, increased attenuation of the gall bladder bile, and subserosal oedema (Fig. 1). Transient, focal, increased attenuation of the liver parenchyma can develop adjacent to the inflamed gall bladder, indicating hepatic arterial hyperaemia and early venous drainage. A combination of these CT findings has a sensitivity comparable to that of sonography in detecting acute cholecystitis **(25).**

Fig. 1 Perforated acute calculous cholecystitis, in a 67-year-old man with acute abdominal pain in the RUQ. MDCT demonstrates an enlarged gall bladder with mural thickening and discontinuity of the medial wall indicative of perforation (*arrow*). In addition, multiple peri-cholecystic abscesses (*arrowheads*) and inflammatory changes in the peri-cholecystic fat are present **(26).**

Dislocation of gallstones in the biliary duct may lead to biliary colic. Patients then often present with recurrent episodes of RUQ pain, fever, and jaundice. The most reliable CT finding is the depiction of the stone within the bilary duct (Fig. 2). MDCT facilitates narrow collimation and multiplanar reconstructions, which may help to detect small calculi in the biliary system, and visualisation of low- and high-attenuated rings allows for identification of mixed cholesterol–calcium stones, often resulting in distal common bile duct obstruction. In the absence of acute pancreatitis or another detectable cause of distal common bile duct obstruction, dislocated gallstone, biliary stricture, and small ampullary mass should be taken into consideration in the differential diagnosis (**27).**

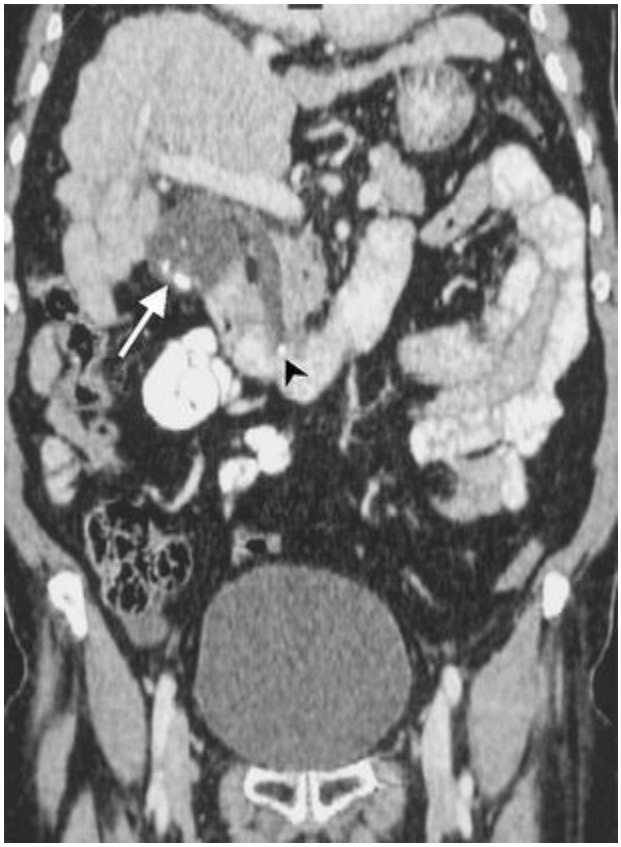

Fig. 2 Biliary obstruction in gallstone disease in a 52-year-old man with acute abdominal pain in the RUQ and liver cirrhosis. Coronal MDCT reconstruction shows multiple calcified stones in the gall bladder (*arrow*) and proximal biliary dilatation secondary to a small obstructing calcified stone in the distal common bile duct (*arrowhead*) **(26).**

Common alternative diagnoses of acute RUQ pain include omental infarction, retrocaecal appendicitis, right-sided diverticulitis, perforated duodenal ulcer, and, rarely, amoebic liver abscess or spontaneous rupture of a hepatic neoplasm.

Left upper quadrant pain

Conditions causing localised pain in the left upper quadrant (LUQ) are rare, with splenic infarction, splenic abscess, sickle cell crisis, and gastric ulcer being the most frequent. In addition, patients with acute pancreatitis can present with LUQ pain.

Common causes of splenic infarction include bacterial endocarditis, portal hypertension, and underlying splenomegaly. On CT, focal infarcts appear as hypodense wedge-shaped areas extending to the splenic surface. Global infarction can result in diffuse hypodensity and can mimic splenic abscess or tumour. For evaluation of splenic pathologies, intravenous administration of contrast medium in an arterial and portal venous phase are recommended. MDCT can improve depiction of surrounding splenic vasculature and associated pancreatic changes by thinner collimation and the use of cine-display **(28).**

Right lower quadrant pain

The most common cause of acute abdominal pain is appendicitis. Although the preoperative diagnosis can be established on the basis of clinical findings, the symptoms of appendicitis may be atypical and mimic other gastrointestinal or genitourinary conditions. Ultrasound is the first-line imaging modality in children and in women of reproductive age, because radiation exposure should be avoided and the small body sizes usually allow for high-quality sonograms. In young women, many causes of right lower quadrant (RLQ) pain are related to gynaecological causes and have to be excluded initially. However, CT is more sensitive than ultrasound in patients

with equivocal presentation. The judicious use of CT in patients with equivocal clinical findings has resulted in a negative appendicectomy rate of 2.5–7% **(29).**

In MDCT, multiplanar viewing provides improved appendiceal visualisation and enhances confidence as to the presence or absence of acute appendicitis (Fig. 3). Coronal reformations are especially useful for visualising the appendix in an unusual location **(29).**

Figure 3 Acute appendicitis and walled-off perforation in a 30-year-old man with fever, elevated white blood cell count, and acute abdominal pain in the RLQ. Coronal reconstructed MDCT depicts the dilated appendix in a retro-ileal position, with circumferential mural enhancement, peri-appendiceal fat stranding, and a small calcified appendicolith in the appendiceal apex (*arrowhead*). Because of extra-luminal gas (*arrow*) one can make the diagnosis of an acute appendicitis with complicating walled-off perforation. This case highlights the use of coronal MPR in identifying the appendix in uncommon anatomical locations **(26).**

Visualisation of a fluid-filled enlarged appendix and focal caecal apical thickening are the most specific CT signs, while peri-appendiceal fat stranding is most sensitive but less specific. Unfortunately, acute appendicitis could also appear without caecal apical thickening or peri-appendiceal fat stranding. Other helpful CT findings include calcified appendicoliths and appendiceal wall enhancement after intravenous administration of contrast agent. However, non-visualisation of the appendix indicates absence of acute appendicitis. The appearance of the abnormal appendix will vary with the degree of inflammation present (**30).**

Recently, new MDCT criteria of the normal appendix have been described. The overall diameter of the normal appendix may vary between 5 mm and 11 mm and is larger than 6 mm in 70%. An appendicolith may be seen in 13%. Despite MDCT, however, 18% of normal appendices were not detected. Preoperative CT not only establishes the diagnosis and depicts unusual appendix location but also helps guide surgical planning. Appendicitis with peri-appendiceal fluid, inflammatory mass, or abscess are good indicators for conversion of laparoscopic to open appendicectomy (**31).**

A number of different protocols for the application of contrast agents is used for evaluating acute appendicitis. Scans can be performed without contrast agent, with orally and intravenously administered contrast agent, with contrast agent applied by oral and colonic routes, and with colonically administered contrast medium

only. Orally and colonically administered contrast materials yield a high diagnostic accuracy as well as the identification of alternative diagnoses in 80% of cases (**32**).

The list of differential diagnoses of RLQ pain is long and includes acute typhlitis, Crohn's disease, caecal diverticulitis, Meckel's diverticulitis (Fig. 4), mesenteric adenitis, right-sided omental infarction, perforated caecal carcinoma, pelvic inflammatory disease, complications of ovarian cysts (torsion, rupture), ectopic pregnancy, or urolithiasis. Non-specific signs seen with appendicitis, such as fat stranding, adjacent bowel wall thickening, and free fluid collection, also occur in these conditions. The identification of a normal appendix is the key to excluding appendicitis (**32**).

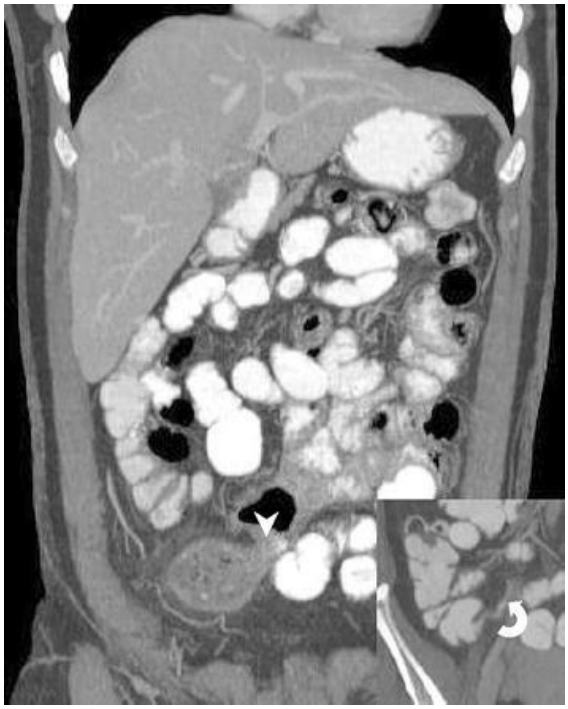

Figure 4 Meckel's diverticulitis in a 48-year-old man with acute abdominal pain in the RLQ. Coronal reconstructed MDCT with maximum-intensity projection demonstrates a dilated diverticulum (*arrowhead*) arising from the small bowel with wall enhancement and adjacent fat stranding, while the appendix, shown in the inlay (*curved arrow*), is normal. These findings are indicative of inflammation of a Meckel's diverticulum **(26).**

Left lower quadrant pain

Diverticular disease is very common in patients older than 65 years, and up to 25% of those patients will develop sigmoid diverticulitis. Clinical misdiagnosis rates range from 34% to 67%. Conversely, MDCT is both sensitive and specific in making a diagnosis of diverticulitis. The most common CT finding of diverticulitis, present in almost 98% of patients, is inflammatory change in the peri-colic fat. Although fat stranding is unspecific, disproportionality, with stranding more severe than expected for the degree of bowel wall thickening, has recently been reported to belong to four main entities: diverticulitis, appendicitis, epiploic appendagitis and omental infarction (**33).**

Other findings include focal colonic wall thickening and free fluid collection. Absence of fat stranding and mural thickening essentially exclude diverticulitis. In advanced disease, peri-colonic inflammation can progress to phlegmon or abscess. CT is the imaging technique of choice for depicting complications, including walled-off perforation, intraperitoneal perforation, fistulae (Fig. 5) and bowel obstruction. With MDCT, narrow collimation facilitates the estimation of stenosis or changes in thickness and contrast of bowel wall. Coronal reformations may provide improved differentiation between normal and abnormal bowel walls. The use of near-isotropic volumes results in reconstructions of imaging planes optimized to the bowel segment in question, or, when curved reconstructions are used, fistulae can be delineated in their entire course (**34).**

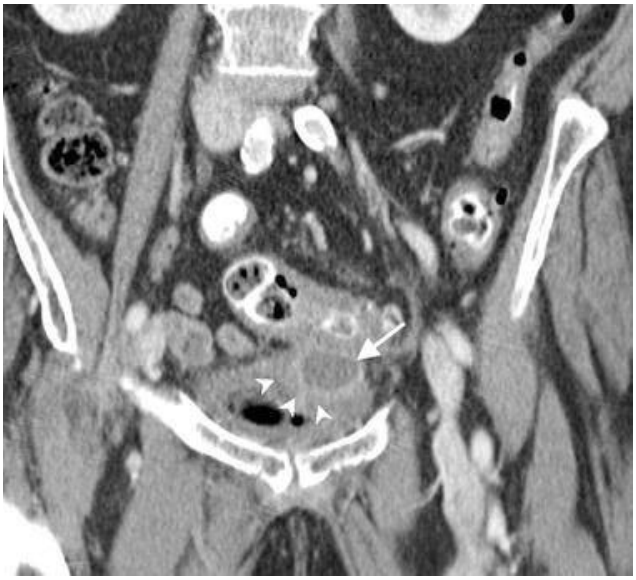

Figure 5 Colovesical fistula in acute diverticulitis in a 74-year-old woman with acute abdominal pain in the left lower quadrant (LLQ) and known diverticular disease. Coronal reconstructed MDCT shows a peri-colonic abscess (*arrow*), adjacent focal bladder wall thickening (*arrowheads*) and air in the bladder, indicating a colovesical fistula in acute diverticulitis **(26).**

Additional benefits of CT include the guidance of therapeutic intervention in complicated forms of diverticular disease and the provision of an alternative diagnosis in patients without diverticulitis. CT-guided drainage of peri-colic or pelvic abscesses can be safely and successfully performed in most patients. However, even a successful drainage should serve as only a temporising measure until an elective surgical resection can be performed **(35).**

Alternative conditions that can clinically mimic sigmoid diverticulitis include colon obstruction secondary to sigmoid carcinoma, gynaecological diseases, or ureteral stone disease. Another alternative diagnosis is primary epiploic appendagitis. Patients with these conditions often lack associated fever or leukocytosis. CT findings are often characteristic, presenting an oval-shaped fatty mass with an associated rim of high attenuation around the periphery of the inflamed appendage, peri-colonic fat streaking, and, occasionally, focal thickening of the adjacent colonic wall (**36).**

Similar CT findings may be present in segmental omental infarction, a condition typically located on the right side and related to obesity and recent surgery. Usage of MPRs for anatomical relation relative to the colon and disproportionality of fat stranding may help in differentiating both entities (**36**).

While most investigators recommend the administration of contrast material only via a rectal enema, intravenous injection of contrast agent is helpful in the detection of peri-colonic inflammation, differentiation of peri-colic abscesses from adjacent bowel loops, and characterisation of pelvic fluid collection. Consequently, if complications are suspected, CT examination should be performed with both colonic and intravenous administration of contrast medium **(37).**

Diffuse abdominal pain

Diffuse abdominal pain is due to irritation of the peritoneum or large portions of the gut and is most frequently caused by infectious or inflammatory bowel disease (IBD), bowel obstruction, acute mesenteric ischemia, and gastrointestinal tract perforation. With increasing use of MDCT in abdominal pain, gastritis and right-sided infectious colitis are diagnosed more often **(38).**

Infectious bowel disease

Gastro-enterocolitis is responsible for approximately 70% of patients with abdominal pain admitted to the emergency department. The vast majority does not require imaging. However, in patients with atypical clinical findings colicky abdominal pain may be the predominant symptom. In those cases, CT may be necessary to differentiate gastro-enterocolitis from alternative diagnoses. At CT, wall thickening with, usually, homogenous enhancement, inflammation of the peri-colic fat, ascites, and multiple air-fluid levels, may be present. Although these findings are non-specific, the portion of colon affected may suggest the presence of a specific organism (**39).**

In patients on potent oral antibiotics, the normal bacterial flora of the colon is disrupted, resulting in the overgrowth of *Clostridium difficile* and causing pseudomembranous colitis. Although non-specific, CT findings include mural thickening, with a halo or target pattern caused by submucosal oedema, peri-colic inflammatory changes, and ascites (Fig. 6). The extent of bowel wall thickening in pseudomembranous colitis is usually greater than in other inflammatory or infectious bowel disease except Crohn's disease (**40).**

As a differentiating point, wall thickening in pseudomembranous colitis is often more irregular than in Crohn's disease. Since pseudomembranous colitis predominantly affects the mucosa and submucosa, peri-colic stranding is often disproportionately mild relative to the colonic wall thickening. Sometimes, contrast material is caught between thickened haustra, producing an accordion-like appearance, which is suggestive of pseudomembranous colitis but typically only occurs in severe cases (**40**).

Figure 6 Pseudomembranous colitis in a 44-year-old man on antibiotics because of meningitis and with acute abdominal pain in the lower abdomen. **a** MDCT scan performed with orally and intravenously administered contrast agent in the portal venous phase demonstrates colonic wall thickening up to 3 cm, low attenuation of bowel wall, and enhancement of luminal surface corresponding to diffuse colonic oedema with mucosal hyperaemia (*arrow*). **b** Sagittal image reveals the ascending colon and right flexure with alternating bands of higher and lower attenuation, an appearance called the accordion sign (*arrowheads*). Because the patient had a history of oral antibiotics use, these CT findings, although not specific, are highly suggestive of *Clostridium difficile*-related colitis **(26).**

Inflammatory bowel disease

The vast majority of patients with chronic IBDs such as ulcerative colitis or Crohn's disease experience chronic symptoms; however, in some patients, acute exacerbation or complications may lead to acute abdominal pain. The diagnostic value of CT is based on the excellent visualisation and documentation of extent and severity of bowel wall inflammation and the estimation of inflammatory activity of the disease. Although there is considerable overlap in the CT findings of ulcerative colitis and Crohn's disease, the location of the involved segment and the extent and appearance of wall thickening may help to distinguish the two. Extensive involvement

of the right colon and small intestine is more common in Crohn's disease, whereas ulcerative colitis is typically left-sided (**41).**

Bowel wall thickening in ulcerative colitis is usually diffuse and symmetric, while wall thickening in Crohn's disease may be eccentric and segmental with skip regions and may result in pseudodiverticula. In addition, the mean wall thickness in Crohn's disease is typically greater than in ulcerative colitis. Proliferation of mesenteric fat and mesenteric lymphadenopathy suggests Crohn's disease rather than ulcerative colitis. On the other hand, the target sign, which represents a low-attenuation ring in the bowel wall due to deposition of submucosal fat, is seen more commonly in ulcerative colitis than in Crohn's disease (**41**).

The use of MPR significantly improves observer confidence in image interpretation, even if additional abnormalities are not revealed. Because CT is able to demonstrate not only the bowel wall but also the surrounding tissue and adjacent structures, CT plays a major role in diagnosing extra-intestinal complications and is the standard technique for guided abscess drainage if ultrasound-guided drainage is not possible (**42).**

Bowel obstruction

Bowel obstruction is a common condition, with the diagnosis based on clinical signs, patient history, and radiographic findings. In order to ensure appropriate treatment, one must determine the site and cause of obstruction and the presence or absence of strangulation. The most commmon causes of small bowel obstruction (SBO) are adhesions because of prior surgery (Fig. 7), Crohn's disease, and tumours. Intussusception is another relatively common cause of SBO in children but is much less frequent in adults (**43)** (Fig. 8).

Figure 7 Adhesive small bowel obstruction in a 43-year-old woman with diffuse acute abdominal pain and a history of kidney transplantation 1 year previously and surgery for anal carcinoma 6 weeks previously. Plain radiography did not provide sufficient information, so a MDCT examination was done and showed distended small bowel loops, measuring more than 2.5 cm in diameter, and collapsed small bowel loops. Coronal reconstructed MDCT clearly detects the transition zone (*arrow*) between distended proximal and collapsed distal bowel loops. Because there is no mass lesion at the transition zone, the diagnosis is adhesive small bowel

obstruction. Open abdominal surgery revealed a fibrous adhesion between small bowel loops, confirming the diagnosis **(26).**

Figure 8 Small bowel intussusception in a 54-year-old man with metastasising malignant melanoma and diffuse acute abdominal pain. Coronal reconstructed MDCT demonstrates a small bowel intussusception with mesenteric fat and vessels in the bowel lumen, resulting in a bowel-within-bowel appearance. The lead point is a jejunal melanoma metastasis (*curved arrow*). Note the additional sub-diaphragmatic metastasis (*arrow*) **(26).**

In large bowel obstruction, the three main causes are carcinoma, diverticulitis, and volvulus (**44).**

Plain radiographs have long been used for confirmation of suspected bowel obstruction. Because of the diagnostic limitations of plain films, CT is increasingly used to identify the site, severity, and underlying cause of obstruction and to determine the presence of complications. CT has an accuracy of up to 96% in cases of high-grade obstruction, while it is less accurate for low-grade SBO (**45).**

The CT hallmark is demonstration of a definable transition from distended to decompressed bowel. Signs of malignant obstruction include mass, lymphadenopathy or abrupt transition with irregular bowel wall thickening. In the absence of a mass or other abnormality in the area of obstruction, adhesions constitute the diagnosis of exclusion in the majority of patients (**45**).

Excellent contrast dynamics and the use of three-dimensional reconstructions render MDCT superior to conventional CT in patients with bowel obstruction. Especially, the determination of the transition point from dilated to non-dilated bowel can be difficult on axial slices alone. Post-processing may enhance detection of the site of obstruction, diagnosis of adhesions, and analysis of the relationship between normal and abnormal bowel wall (**45**).

CT is also very helpful in differentiating between simple and closed-loop bowel obstruction. Closed-loop obstruction, often secondary to adhesion or hernia, is characterised by mechanical bowel obstruction in which two points along the course of the bowel are obstructed at a single site. Characteristic CT findings are a C-shaped, U-shaped, or “coffee-bean” configuration of the bowel loop. Other findings suggestive of strangulation include fluid in the mesenteric leaves radiating out from the point of strangulation and the “whirlpool sign”, caused by the

twisting of the bowel, with local engorgement of mesenteric vessels, mesenteric oedema, and bowel thickening (**43).**

In addition, because of its superior anatomical detail, MDCT may potentially detect subtle signs of strangulation, such as mesenteric stranding, poor bowel wall enhancement, wall thickening, and free air or fluid (**38).**

In the differentiation of mechanical obstruction from paralytic ileus, CT has been reported to be highly accurate. Paralytic ileus is due to paralysis of the gut musculature and is a common problem in the postoperative period or may be secondary to ischaemic conditions, inflammatory or infectious disease, abnormal metabolic drug or hormone levels, or innervation defects. CT can demonstrate involved bowel segments and may be helpful in determining the underlying cause (**46**).

Ischaemic bowel disease

Ischaemic bowel disease shows a broad spectrum of clinical and radiological manifestations, ranging from transient ischaemia to necrosis of large portions of the bowel. Common causes of acute mesenteric ischaemia are embolic arterial occlusion, usually of cardiac origin, non-occlusive ischaemia, and, less frequently, superior mesenteric vein thrombosis, vasculitis, or dissection of the superior mesenteric artery. In previous studies, CT has been shown to be very useful for the diagnosis of bowel ischaemia. Typical CT findings of bowel ischaemia—although non-specific—include bowel dilatation and wall thickening, abnormal bowel wall enhancement, intestinal pneumatosis, and ascites (**47**).

By evaluating the mesenteric vasculature, CT may sometimes be able to detect the underlying cause, such as atherosclerotic plaques, thrombus or occlusion (Fig. 9). MDCT facilitates the investigation of a true arterial phase of enhancement before opacification of adjacent veins, and thin-collimated reformations for better depiction of small vessels are recommended. We routinely perform dual-phase imaging to allow us to evaluate both arterial and venous patency as well as to define the pattern of bowel wall and parenchyma enhancement. Evaluation of axial images and multiplanar display are usually sufficient for detecting alterations of the bowel wall and the main mesenteric vessels, while VR images have the advantage of demonstrating mesenteric vessels, from their origin to distal branches, on a single projection (**48).**

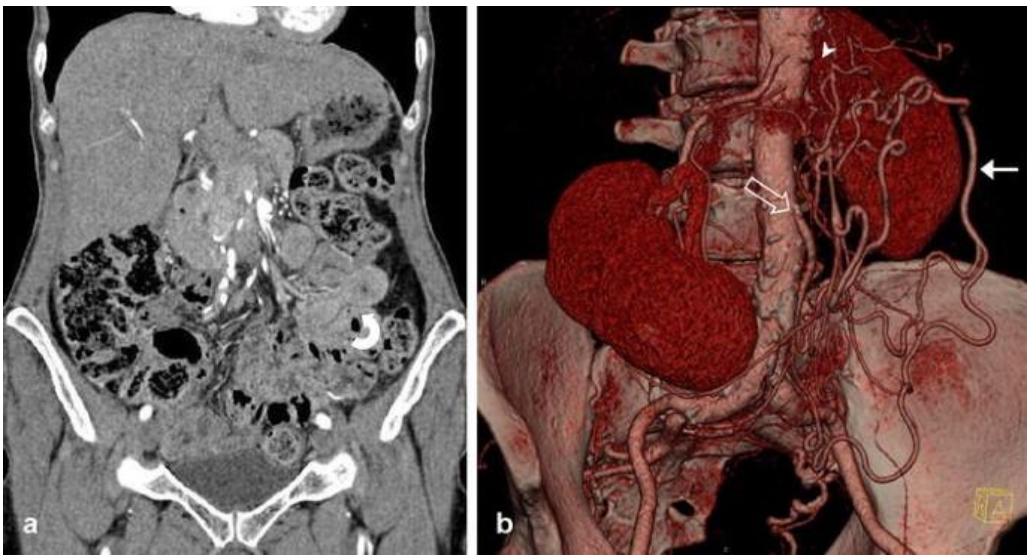

Figure 9 Ischaemic bowel disease secondary to generalised arteriosclerosis in a 64-year-old woman with severe diffuse abdominal pain. **a** Coronal MDCT reconstruction shows thickening and heterogeneous enhancement of several small bowel loops (*curved arrow*). **b** Volume-rendered image delineates an occlusion of the superior mesenteric artery (*arrowhead*) and a high-grade stenosis of the inferior mesenteric artery (*open arrow*). Note the collateralisation through the dilated arc of Riolan (*arrow*) **(26).**

Non-occlusive mesenteric ischaemia (NOMI) is commonly caused by decreased cardiac output, resulting in splanchnic hypoperfusion. Typical angiographic signs, including narrowing and vasoconstriction of multiple branches of the superior mesenteric artery, alternate dilatation and narrowing of intestinal branches, spasms of mesenteric arcades, impaired filling or occlusion of intramural vessels, reflux of contrast agent into the abdominal aorta, and spread-out segmental arteries due to distension of bowel loops, are sometimes difficult to depict on CT angiography. Typical CT findings of bowel ischaemia in the setting of normally perfused mesenteric vessels then may facilitate the diagnosis of NOMI (**48).**

Gastrointestinal tract perforation

Gastrointestinal tract perforation may be found complicating appendicitis, diverticulitis, peptic ulcer disease, or following endoscopic procedures, particularly endoscopic biopsy or polypectomy. CT is the most reliable diagnostic method to assess gastrointestinal perforation, as it allows detection of even small amounts of free air in the abdomen as a sign of perforation (**49).**

Viewing on a "lung window" setting may enhance the sensitivity of detecting subtle extra-luminal gas. Although evaluation could be made on non-enhanced CT examination, oral and intravenous administration of contrast is recommended for localisation of the site of perforation and for diagnosing the underlying cause. The localisation of extra-luminal air varies, depending on the position of the patient, and is usually not identical with the site of perforation. Helpful CT signs for localisation may be focal fluid, extravasation of orally administered contrast material, and local inflammatory changes (**49).**

Acute pancreatitis

In acute pancreatitis, CT findings correlate well with the severity of disease. Consequently, CT is the imaging modality of choice to classify pancreatitis and to detect complications such as pseudoaneurysms, porto-mesenteric venous occlusion, pseudocysts, or abscess (Fig. 10) (**50).**

Fig. 10 Acute necrotising pancreatitis in a 69-year-old man with severe acute epigastric pain. Serial MDCT images show an enlarged pancreas and large, sharply demarcated, areas within the pancreatic parenchyma lacking enhancement (*arrows*). Note the small fluid collections in the anterior pararenal space (*arrowheads*) and the thickening of Gerota's fascia (*open arrow*). These CT findings are indicative of acute necrotising pancreatitis of the head and body of the pancreas. The tail is almost unaffected (*asterisk*) **(26).**

In mild forms, CT shows a peri-pancreatic inflammatory exudate and an otherwise normal appearing or homogeneously enlarged gland. In up to 28% of patients with mild pancreatitis, the results of CT examination may be normal (**50).**

In severe forms, small intrapancreatic fluid collections are present as a result of intraglandular necrosis. Necrotising pancreatitis exhibits necrotic regions as unenhanced areas sharply demarcated from normally enhancing parenchyma. Peri-pancreatic exudates may penetrate along fascial planes and extend to adjacent organs. Fluid collections typically accumulate in the anterior pararenal space, lesser sac, mesenteric root, and transverse mesocolon. The thinner collimation of MDCT reveals vascular complications such as pseudoaneurysms or thrombosis of the splenic and portal veins. Because of the rapid image acquisition time with MDCT, vascular contrast phases can be clearly separated **(51).**

Arterial phase imaging allows direct visualisation of arterial branches without opacification of adjacent veins. Portal venous phase imaging facilitates evaluation of pancreatitis and associated complications such as venous thrombosis. Curved planar reformations are useful in displaying the whole tortuous pancreas, tracing the cholangiopancreatic duct and peri-pancreatic vessels and highlighting the relationship of lesions with surrounding anatomical structures (**52).**

Advantages of MDCT

The evolution from single-slice CT to current MDCT scanners has resulted in several important advantages. First, the shortened acquisition time increases scanner productivity and reduces motion artefacts by scanning the entire abdomen in a single breath-hold, which is essential in acutely ill patients (**53**). Second, thin collimation enables sub-millimetre isotropic imaging, permitting reconstructions in any arbitrary plane with a spatial resolution similar to that of the axial plane. Third, better contrast bolus exploitation allows precise separation of multiple phases of enhancement, which is especially useful in the evaluation of vascular diseases. Furthermore, increased computing speed of state-of-the-art workstations has shortened reconstruction times, facilitating faster radiological interpretation (**53**).

References:

1. Dubuisson, V., Voïglio, E., Grenier, N., et al. (2015). Imaging of non-traumatic abdominal emergencies in adults. Journal of Visceral Surgery, 152(6), S57–S64. https://doi.org/10.1016/j.jviscsurg.2015.09.006
2. Chaurasia, R., & Kumar, P. (2022). Role of computed tomography in non-traumatic acute abdomen in adults. Asian Journal of Medical Sciences, 13(11), 232–237. https://doi.org/10.3126/ajms.v13i11.45440
3. Rao, M. S., Reddy, K. J., Ramanappa, M., et al. (2014). Evaluation of non-traumatic acute abdomen. Indian Journal of Mednodent and Allied Sciences, 2(2), 131–137.
4. Romans L. (2018). Computed Tomography for Technologists: A Comprehensive Text. Wolters Kluwer Health.
5. Chinene B. (2022). Multi-Detector Computerized Tomography (MDCT): Principles and Applications. 10.13140/RG.2.2.36381.59362.
6. Ko BS, Wong DT, Cameron JD, et al., (2014). 320-row CT coronary angiography predicts freedom from revascularisation and defers invasive angiography in stable CAD: a fractional flow reserve–correlated study. Eur Radiol. 24:738–747.
7. Parakh A, Kortesniemi M, Schindera ST. (2016). CT radiation dose management: a comprehensive optimization process for patient safety. Radiology. 280(3).
8. Sodickson A. (2012). Strategies for reducing radiation exposure in multi-detector row CT. Radiol Clin North Am. 50(1):1–14.
9. Bushong SC. (2013). Radiologic Science for Technologists: Physics, Biology, and Protection. Elsevier Mosby. ISBN: 978-0-323-08135-1.
10. Greffier J, Pereira F, Macri F, et al., (2016). CT dose reduction using Automatic Exposure Control and iterative reconstruction: A chest paediatric phantoms study. Phys Med. 32(4):582-589.
11. MacDougall RD, Kleinman PL, Callahan MJ. (2016). Size-based protocol optimization using automatic tube current and kV modulation in CT. J Appl Clin Med Phys. 17(1).

12. Martin CJ, Sookpeng S. (2016). Setting up CT automatic tube current modulation systems. J Radiol Prot. 36:R74–R95.
13. Speelman A, Davidson R. (2006). Does low dose CT compromise detection of hepatic metastases? South African Radiographer. 44(02).
14. Liu F, Yang Q, Cong W, et al., (2014). Dynamic Bowtie Filter for Cone-Beam/MultiSlice CT. PLoS ONE. 9(7):e103054.
15. Yee J, Dachman A, Kim DH, et al., (2024). CT colonography reporting and data system (C-RADS): version 2023 update. Radiology. 310(1):e232007.
16. Svensson MH, Svensson E, Lasson A, et al., (2002). Patient acceptance of CT colonography vs. colonoscopy. Radiology.
17. González-Suárez B, Pagés M, Araujo IK, et al., (2020). Colon capsule endoscopy versus CT colonography in FIT-positive colorectal cancer screening subjects: the VICOCA trial. BMC Med. 18:255.
18. Mørup SD, Precht H, Foley S, et al., (2019). Impact of decentring patients for abdominal CT scan. Insights Imaging. 10(Suppl 1):326.
19. Yamagishi M, Tamaki N, Akasaka T, et al., (2021). JCS 2018 guideline on diagnosis of chronic coronary heart diseases. Circ J. 85(4):402–572.
20. Onur MR, Özbay Y, İdilman İ, t al., (2023). Abdominal CT findings in COVID-19: a multicenter study. Diagn Interv Radiol. 29(3):414.
21. Eltatawy DN, Elsharawy FA, Elbarbary AA, et al., (2021). Multi-detector computed tomography (MDCT) as a diagnostic tool in assessment of thoracic aortic anomalies in pediatric patients. Egypt J Radiol Nucl Med. 52:39.
22. Stengel D, Leisterer J, Ferrada P, et al., (2018). Point-of-care ultrasonography for diagnosing thoracoabdominal injuries in blunt trauma patients. Cochrane Database Syst Rev. 12:CD012669.
23. Kataria B, Woisetschläger M, Althén JN, et al., (2024). Image quality assessments in abdominal CT: Relative importance of dose, iterative reconstruction strength and slice thickness. Radiography. 30(6):1563-1571.
24. Khafaji MA, Bagasi JT, Albahiti SK, et al., (2023). Accuracy of Ultrasound and CT in Diagnosing Acute Cholecystitis in a Saudi Tertiary Care Center. Cureus. 15(9):e44934.
25. Yeo DM, Jung SE. (2018). Differentiation of acute vs chronic cholecystitis using MDCT. Medicine. 97(33):66–78. https://doi.org/10.1097/MD.0000000000011851
26. Leschka S, Alkadhi H, Wildermuth S, et al., (2005). Multi-detector CT of the acute abdomen. Eur Radiol. 15:2435–2447.
27. McNicoll CF, Pastorino A, Farooq U, et al., (2023). Choledocholithiasis. In: StatPearls [Internet]. Treasure Island (FL): StatPearls Publishing.
28. Gourtsoyianni S, Laniado M, Ros-Mendoza L, et al., (2023). The spectrum of solitary benign splenic lesions—Imaging clues for a noninvasive diagnosis. Diagnostics. 13(12):2120.
29. Wonski S, Ranzenberger LR, Carter KR. (2023). Appendix Imaging. In: StatPearls [Internet]. Treasure Island (FL): StatPearls Publishing.
30. El-Badrawy A, Shebel H, El Atta HMA. (2022). MDCT diagnosis of synchronous primary gastrointestinal tract carcinoma and other solid malignancies: case series study. Egypt J Radiol Nucl Med. 53:34.
31. Althobaiti E, Mirza R, Brinji A, et al., (2023). Oral Contrast in Diagnosing Acute Appendicitis; Is It Necessary? Saudi Journal of Radiology. 2(1): 38–47.
32. Munie ST, Nalamati SPM. (2018). Epidemiology and Pathophysiology of Diverticular Disease. Clin Colon Rectal Surg. 31(4):209–213.
33. Tiralongo F, Di Pietro S, Milazzo D, et al., (2023). Acute colonic diverticulitis: CT findings, classifications, and a structured reporting template. Diagnostics. 13(24):3628.
34. Vaccaro C, Avellaneda N. (2023). Surgical Management of Complicated Diverticulitis. In: Diverticular Bowel Disease—Diagnosis and Treatment. IntechOpen.
35. Pulzato I, Boero E, Shaipi E, et al., (2019). Sigmoid diverticulitis mimicking cholecystitis: a clinical challenge. Ultrasound J. 11:14.

36. Biondi M, Bicci E, Danti G, et al., (2022). The role of magnetic resonance enterography in Crohn's disease: a review of recent literature. Diagnostics. 12(5):1236.
37. Davarpanah AH, Ghamari Khameneh A, Khosravi B, et al., (2021). Many faces of acute bowel ischemia: overview of radiologic staging. Insights Imaging. 12:56.
38. Choi SY. (2021). Comparison of Clinical Characteristics According to the Existence of Secondary Appendicitis in Pediatric Acute Enterocolitis: A Single Center Study. Pediatr Gastroenterol Hepatol Nutr. 24(2):127-134.
39. Mada PK, Alam MU. (2024). Clostridioides difficile infection. In: StatPearls [Internet]. Treasure Island (FL): StatPearls Publishing.
40. Ranasinghe IR, Tian C, Hsu R. (2024). Crohn Disease. In: StatPearls [Internet]. Treasure Island (FL): StatPearls Publishing.
41. van Harten LD, de Jonge CS, Beek KJ, et al., (2022). Untangling and segmenting the small intestine in 3D cine-MRI using deep learning. Med Image Anal. 78:102386.
42. Muldoon RL. (2021). Malignant Large Bowel Obstruction. Clin Colon Rectal Surg. 34(4):251-261.
43. Nelms DW, Kann BR. (2021). Imaging Modalities for Evaluation of Intestinal Obstruction. Clin Colon Rectal Surg. 34(4):205-218.
44. Beach EC, De Jesus O. (2023). Ileus. In: StatPearls [Internet]. Treasure Island (FL): StatPearls Publishing.
45. Monita MM, Gonzalez L. (2023). Acute Mesenteric Ischemia. In: StatPearls [Internet]. Treasure Island (FL): StatPearls Publishing.
46. Ronza FM, Di Gennaro TL, Buzzo G, et al., (2024). Diagnostic Role of Multi-Detector Computed Tomography in Acute Mesenteric Ischemia. Diagnostics. 14(12):1214.
47. Pouli S, Kozana A, Papakitsou I, et al., (2020). Gastrointestinal perforation: clinical and MDCT clues for identifying aetiology. Insights Imaging. 11:31.
48. Mohey N, Hassan TA. (2020). Correlation between modified CT severity index and retroperitoneal extension via interfascial planes in suspected acute severe pancreatitis. Egypt J Radiol Nucl Med. 51:81.
49. Jiang ZQ, Xiao B, Zhang XM, et al., (2021). Early-phase vascular involvement is associated with acute pancreatitis severity: a magnetic resonance imaging study. Quant Imaging Med Surg. 11(5):1909.
50. McCollough CH, Rajiah PS. (2023). Milestones in CT: Past, Present, and Future. Radiology. 309(1):e230803.